Journal of Applied Physics

Optical properties and electric field enhancement in cholesteric liquid crystal containing different periodicities

Cite as: J. Appl. Phys. **100**, 023102 (2006); https://doi.org/10.1063/1.2215124
Submitted: 25 October 2005 . Accepted: 24 May 2006 . Published Online: 17 July 2006

Ryotaro Ozaki, Yuko Matsuhisa, Hiroyuki Yoshida, Katsumi Yoshino, and Masanori Ozaki

Optical properties and electric field enhancement in cholesteric liquid crystal containing different periodicities

Ryotaro Ozaki,[a] Yuko Matsuhisa, Hiroyuki Yoshida, Katsumi Yoshino, and Masanori Ozaki[b]
Division of Electrical, Electronic and Information Engineering, Osaka University, 2-1 Yamada-Oka, Suita, Osaka 565-0871, Japan

(Received 25 October 2005; accepted 24 May 2006; published online 17 July 2006)

We study a defect mode in a one-dimensional photonic band gap of a cholesteric liquid crystal (CLC) consisting of two helicoidal periodicities. The optical properties of this CLC are analyzed using 4×4 transfer matrix and finite difference time domain (FDTD) methods. In calculated transmission spectra of this CLC, one of the defect modes always appears at the band edge wavelength of the inner CLC having a different helix to that of two sides of CLCs. Furthermore, the electric field analysis of this CLC has also been demonstrated by the FDTD method. At the defect mode wavelength, the electric field enhancement is found to be significant larger than a normal CLC. © *2006 American Institute of Physics*. [DOI: 10.1063/1.2215124]

I. INTRODUCTION

Photonic crystals (PCs) having three-dimensional ordered structure with a periodicity of optical wavelength have attracted considerable attention from both fundamental and practical point of view, because in such materials, a photonic band gap exists in which the existence of a certain energy range of photon is forbidden, and various applications of PCs have been proposed.[1,2] In particular, the study of stimulated emission in the photonic band gap is one of the most attractive subjects, since, in the band gap, a spontaneous emission is inhibited and low threshold lasers based on photonic crystals are expected. In a one-dimensional (1D) periodic structure, laser action has been expected at the photonic band edge where the photon group velocity approaches zero.[3] A localization of light based on a defect mode caused by an imperfection in a periodic structure has also been expected to be applied to the fabrication of low threshold lasers and microwaveguides. Recently, we have demonstrated the tunable 1D PC lasers using liquid crystals (LCs) having a large optical anisotropy.[4,5]

On the other hand, liquid crystals including chiral molecules have a self-organized helical structure which can be regarded as a 1D periodic structure. The so-called stop band in which light cannot propagate, which is considered a 1D pseudo-band-gap, exists in such systems. Lasing at the band edge has been reported in cholesteric liquid crystals (CLCs), chiral smectic LCs, and polymerized CLCs.[6–9] In chiral LCs, several new types of defect modes have been proposed. For example, the introduction of an isotropic defect layer into a periodic helical structure of CLC has been theoretically studied.[10] From the concept of phase jump, the existence of a twist defect, which is a discontinuous point of a periodic helical structure, has been predicted.[11] We have experimentally demonstrated the defect mode in a 1D photonic band gap of the CLC having a twist defect using photopolymerized CLC (PCLC) films.[12] The laser action based on the twist defect mode has also been observed in the dye-doped PCLC composite film with the twist defect. The defect mode caused by a partial deformation of a helix in a CLC has been proposed.[13] In this model, an optically induced local modulation of helical twisting power is used as a method of inducing the helix defect, which can be achieved by photochemical effects. In a hybrid system consisting of nematic and cholesteric LCs, a phase retardation defect has been demonstrated by the introduction of a nematic LC defect layer into a PCLC.[14]

In this study, we have investigated a defect mode in a 1D photonic band gap of a CLC consisting of two helicoidal periodicities. The optical properties of this CLC have been analyzed by calculating the electromagnetic wave transmission. Furthermore, we have also discussed the electric field enhancement in the CLC containing different periodicities.

II. METHOD OF ANALYSIS

Figure 1 shows a schematic view of the CLC consisting of two helicoidal periodicities. In this study, the two sides and center parts of this CLC are defined as CLC_1 and CLC_2, respectively. The pitch length of the CLC_2 is shorter than that

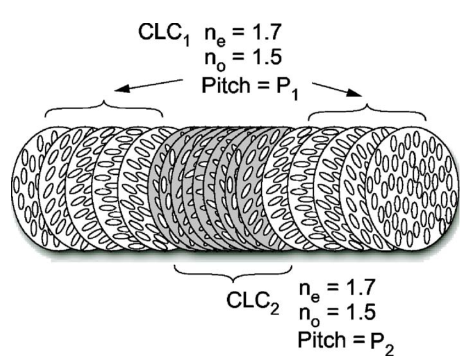

FIG. 1. Schematic view of cholesteric liquid crystal (CLC) containing different periodicities.

[a]Electronic mail: ozaki@nda.ac.jp
[b]Electronic mail: ozaki@eei.eng.osaka-u.ac.jp

of the CLC_1, but their refractive indices are the same. Therefore, the CLC_2 differs from the CLC_1 only in helical pitch length.

In order to investigate the optical properties of these CLCs, we have performed a theoretical calculation of the light propagation in the CLC consisting of two helicoidal periodicities using a 4×4 matrix. This method is a numerical analysis of Maxwell equations that enable the quantitative calculation of the light propagation in a medium with a refractive index varying along one direction.[15] The light propagating along the z axis with the frequency ω is given by

$$\frac{d\Psi(z)}{dz} = \frac{i\omega}{c} D(z)\Psi(z), \tag{1}$$

where $D(z)$ is a derivative propagation matrix and $\Psi(z) = (E_x, H_y, E_y, H_x)^T$. From this equation, we can obtain transmission and reflection properties.

We have also calculated the electric field distribution in the CLC consisting of two helicoidal periodicities by the finite difference time domain (FDTD) method. This method is an analysis of Maxwell equations based on the Yee algorithm in discrete time and lattices.[16] When the Maxwell equations of the electromagnetic field propagating in an anisotropic medium along the z axis are approximated by finite differences, we obtain

$$E_x^{t+1}(i) = -\frac{\varepsilon_{yy}}{\varepsilon'}\frac{\Delta t}{\Delta z}\{H_y^T(j+1) - H_y^T(j)\} - \frac{\varepsilon_{xy}}{\varepsilon'}\frac{\Delta t}{\Delta z}\{H_x^T(j+1) - H_x^T(j)\} + E_x^t(i), \tag{2a}$$

$$E_y^{t+1}(i) = \frac{\varepsilon_{xx}}{\varepsilon'}\frac{\Delta t}{\Delta z}\{H_x^T(j+1) - H_x^T(j)\} + \frac{\varepsilon_{xy}}{\varepsilon'}\frac{\Delta t}{\Delta z}\{H_y^T(j+1) - H_y^T(j)\} + E_y^t(i), \tag{2b}$$

$$H_x^{T+1}(j) = -\mu_0\frac{\Delta t}{\Delta z}\{E_y^t(i+1) - E_y^t(i)\} + H_x^T(i), \tag{2c}$$

$$H_y^{T+1}(j) = -\mu_0\frac{\Delta t}{\Delta z}\{E_x^t(i+1) - E_x^t(i)\} + H_y^T(i), \tag{2d}$$

$$\varepsilon' = \varepsilon_{xx}\varepsilon_{yy} - 2\varepsilon_{xy}, \tag{2e}$$

where Δz related to the resolution of the calculation is 1 nm. The following first-order absorbing boundary condition is used at the boundaries of the system. A sinusoidal point optical source is used as excitation source to incident light into a cell.

III. RESULTS AND DISCUSSION

Figure 2 shows the calculated transmission spectra of the single and composite CLCs. The single CLC is a normal CLC which does not have a helix deformation, and the composite CLC is a CLC consisting of two helicoidal periodicities as shown in Fig. 1. The broken lines in Fig. 2 show the calculated transmission spectra of the single CLC_1 and CLC_2. The CLC_1 and CLC_2 have right-handed helices, and an incident light is circularly polarized with the same sign of

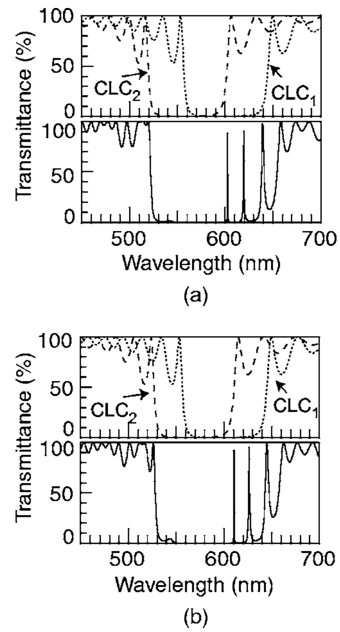

FIG. 2. Transmission spectra of the single CLC and composite CLC as a function of the pitch length of the CLC_2. The pitch lengths of the CLC_2 are (a) 350 nm and (b) 355 nm. The upper graph shows transmission spectra of the single CLC_1 and single CLC_2. The lower graph shows transmission spectra of the CLCs consisting of the CLC_1 and CLC_2.

rotation of the CLC. The numbers of helical pitches of both the CLC_1 and CLC_2 are 10, and their ordinary and extraordinary refractive indices are 1.5 and 1.7, respectively. In Figs. 2(a) and 2(b), the pitch length of the CLC_1 is constant at 375 nm, but these of the CLC_2s are (a) 350 nm and (b) 360 nm. The difference between the CLC_1 and CLC_2 is only in the pitch length. Under this condition, the stop bands of about 80 nm spectral widths are observed in transmission spectra, and those of the CLC_1 and CLC_2 overlap.

The solid lines in Fig. 2 show the calculated transmission spectra of the composite CLC shown in Fig. 1. In this composite CLC, the pitch number of the CLC_2 at center and that of the CLC_1 on one side are 10 and 5, respectively. Since this composite CLC is composed of different pitches, a wide stop band appears in the transmission spectrum. In addition, the defect mode peaks caused by the introduction of the CLC_2 layer appear in the stop band. The defect mode peaks exist with the exception of the band gap of the CLC_2 because the incident light is reflected by the CLC_2. It should be noted that the defect mode peaks under any condition appear at the band edge wavelength of the CLC_2. In general, a light propagating through a 1D PC with a defect layer is reflected at band gap wavelength, and the lights can propagate at the defect mode wavelength. This is because a phase matching condition is satisfied at the defect mode wavelength. The phase matching condition depends on an optical length or a phase retardation of a defect layer. In the composite CLC, however, one of defect modes always appears at the band edge wavelength of the CLC_2. This is explained by the phase matching condition and by coupling between the band edge mode of CLC_2 and the defect mode of CLC_1 resonator. The incident light passing through the CLC_1 feels the periodicity of the CLC_2. When the incident light wavelength is the band

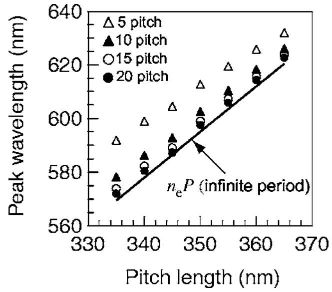

FIG. 3. Defect mode wavelengths at the CLC_2 band edge wavelength as functions of the pitch length of and pitch number of the CLC_2.

edge of the CLC_2, the propagating light in the CLC_2 produces a standing wave of band edge mode caused by matching between the periodicity of inner CLC_2 and the incident light wavelength. Since the standing wave consists of the multiple of the half wavelength of the incident light, the standing wave at the both ends of the inner CLC_2 is wave node. Even if the pitch length changed, the light at the both ends of the CLC_2 becomes wave node at the CLC_2 band edge wavelength because the standing wave of band edge mode is formed by the integral multiple of the half wavelength. In any pitch length, therefore, the standing wave appears at the CLC_2 band edge wavelength. These indicate that the inner CLC_2 band edge wavelength always satisfies the phase matching condition for resonance, and that the standing wave of band edge mode is coupled with the defect mode of CLC_1 resonator. As a result, the light at the band edge of the CLC_2 propagates through the composite CLC and the defect mode appears at the band edge wavelength of CLC_2. In other words, the coupled defect mode peak indicates the band edge wavelength of the inner CLC_2 in a different form.

For a verification of the association between the coupled defect mode and the inner band edge, we also calculated the defect mode wavelength in the CLC consisting of different periodicities. Figure 3 shows the defect mode wavelength in the composite CLC, as functions of the pitch length of and pitch number of CLC_2. The defect mode peaks in the composite CLCs shift to longer wavelength with elongations of the pitch lengths. These shifts arise in the same manner as any conditions. In Fig. 3, the solid line represents the band edge of lower energy state of the CLC_2 consisting of an infinite periodicity, which is given by the product of the extraordinary refractive index n_e and the pitch length P, i.e., $\lambda = n_e P$. The defect mode wavelengths near the band edge of the infinite periodic structure with the increase of the pitch number. These shifts are similar to a change of a band edge of a single CLC. In order to illustrate, Fig. 4 shows transmission spectra of 5- and 20-pitch single CLCs. In the five-pitch CLC, the transmission within the stop band does not fall to 0%, and band edges are not sharp. These are caused by that the periodicity is not enough to reflect lights. But, the more pitch number increases, the sharper the band edge becomes. The band edge nears the $n_e P$ with the increase of the pitch number, as shown in Fig. 4. These results correspond to the coupled defect mode in the composite CLC shown in Fig. 3.

In order to investigate the enhancing effect of the coupled defect mode, we have performed theoretical calculation of the electric field distribution in the composite CLC by using the FDTD method. For comparison, those in a single CLC_2 and in a CLC_1 with an isotropic defect have also been calculated. Figure 5(a) shows the electric field distribution in the composite CLC at the band edge wavelength of the CLC_2, where the pitch lengths of the CLC_1 and CLC_2 are 375 and 350 nm, and the pitch numbers of the CLC_1 and CLC_2 are 10 and 15, respectively. Figure 5(b) shows the electric field distribution in the CLC_1 with the isotropic defect layer at defect mode wavelength. The length of the iso-

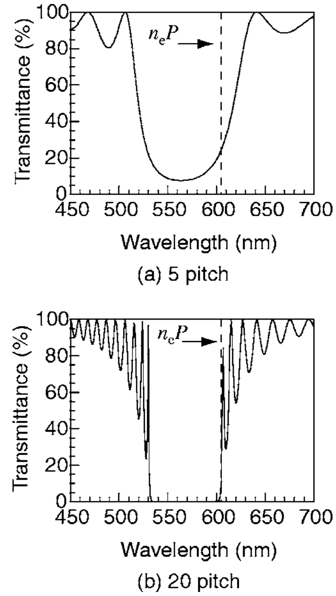

FIG. 4. Transmission spectra of 5- and 20-pitch single CLCs.

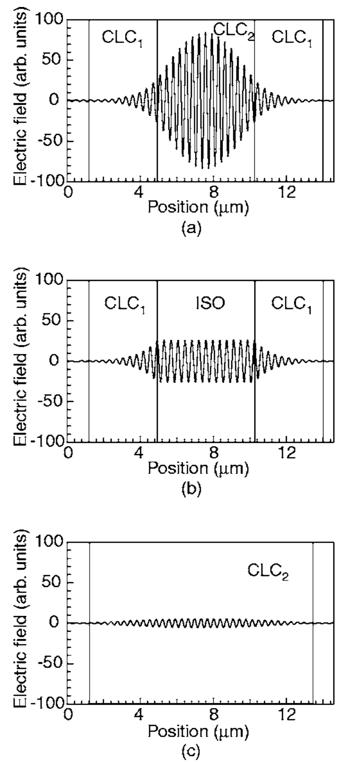

FIG. 5. Electric field distributions of (a) CLC containing different periodicities, (b) CLC_1 with an isotropic defect layer, and (c) single CLC_2.

tropic defect layer is the same as the CLC_2 layer of Fig. 5(a), and the refractive index of the isotropic layer is 1.6. This refractive index is an average of the ordinary and extraordinary indices of CLC_2. Figure 5(c) shows the electric field distribution in the single CLC_2 at band edge wavelength. For comparison with same pitch number, the 25-pitch single CLC_2 was calculated. In these calculations, the incident lights are circularly polarized and have the same sign of rotation of the CLC helix. It should be noted that the electric field in the composite CLC shown in Fig. 5(a) is amplified significantly. Of the three configurations, the electric field enhancement in the composite CLC is the highest, followed in order by the CLC_1 with the isotropic defect and the single CLC_2. Compared with the single CLC_2 and the CLC_1 with the isotropic defect, the electric field in the isotropic defect is larger than that of single CLC_2, because of the light in the isotropic defect is confined in the smaller space. In addition, the electric field in the isotropic defect is enhanced by using a high reflection region in the stop band of the CLC_1, but the electric field enhancement in the single CLC is caused by a small amount of refractive index change of the CLC_2. On the other hand, the reason why the enhancement of the composite CLC is larger than that of the CLC with the isotropic defect is as follows. In the isotropic defect system, the defect layer is used as just a path for propagating lights. In contrast, the electric field in the composite CLC is not only enhanced by the defect mode of the CLC_1 resonator but also the band edge mode of the inner CLC_2. Therefore, in the composite CLC, lights are enhanced further by the multiplier effects of the CLC_1 and the CLC_2.

IV. CONCLUSIONS

We studied the optical properties of the CLC consisting of two helicoidal periodicities using the 4×4 matrix and FDTD methods. In the composite CLC, one of the defect mode peaks always appeared at the band edge wavelength of the CLC_2. This is because the incident light propagating in the CLC_2 was not canceled out due to the periodicity of the CLC_2. In other words, the defect mode peak indicates the band edge wavelength of the inner CLC. Furthermore, the electric field enhancement at the defect mode is significant larger than a normal CLC. This is because lights in the composite CLC are enhanced by the multiplier effect of the CLC_1 and the CLC_2. This high enhancement is expected as potential applications such as a nonlinear optics and low-threshold laser.

ACKNOWLEDGMENTS

This work is supported by a Grant-in-Aid for Scientific Research from the Japan Ministry of Education, Culture, Sports, Science and Technology.

[1] E. Yablonovitch, Phys. Rev. Lett. **58**, 2059 (1987).
[2] S. John, Phys. Rev. Lett. **58**, 2486 (1987).
[3] J. P. Dowling, M. Scalora, M. J. Bloemer, and C. M. Bowden, J. Appl. Phys. **75**, 1896 (1994).
[4] R. Ozaki, T. Matsui, M. Ozaki, and K. Yoshino, Appl. Phys. Lett. **82**, 3593 (2003).
[5] R. Ozaki, Y. Matsuhisa, M. Ozaki, and K. Yoshino, Appl. Phys. Lett. **84**, 1844 (2004).
[6] V. I. Kopp, B. Fan, H. K. M. Vithana, and A. Z. Genack, Opt. Lett. **23**, 1707 (1998).
[7] M. Ozaki, M. Kasano, D. Ganzke, W. Haase, and K. Yoshino, Adv. Mater. (Weinheim, Ger.) **14**, 306 (2002).
[8] H. Finkelman, S. T. Kim, A. Munoz, and P. Palffy-Muhoray, Adv. Mater. (Weinheim, Ger.) **13**, 1069 (2001).
[9] T. Matsui, R. Ozaki, K. Funamoto, M. Ozaki, and K. Yoshino, Appl. Phys. Lett. **81**, 3741 (2002).
[10] Y.-C. Yang, C.-S. Kee, J.-E. Kim, H. Y. Park, J.-C. Lee, and Y.-J. Jeon, Phys. Rev. E **60**, 6852 (1999).
[11] V. I. Kopp and A. Z. Genack, Phys. Rev. Lett. **89**, 033901 (2002).
[12] M. Ozaki, R. Ozaki, T. Matsui, and K. Yoshino, Jpn. J. Appl. Phys., Part 2 **42**, L472 (2003).
[13] M. H. Song *et al.*, Adv. Mater. (Weinheim, Ger.) **16**, 779 (2004).
[14] T. Matsui, M. Ozaki, and K. Yoshino, Phys. Rev. E **69**, 061715 (2004).
[15] D. W. Brerreman, J. Opt. Soc. Am. **63**, 1374 (1973).
[16] K. S. Yee, IEEE Trans. Antennas Propag. **14**, 302 (1966).